Chapter 4. Graphitic carbon nitride-titanium dioxide nanocomposite for photocatalytic hydrogen production under visible light

Mohammad Reza Gholipour,[a] François Béland[b] and Trong-On Do[a,*]

[a] Department of Chemical Engineering, Université Laval, Québec, G1V 0A6, Canada

[b] SiliCycle Inc., 2500, Boul. du Parc-Technologique

Québec (QC) G1P 4S6, Canada.

International Journal of Chemical Reactor Engineering, **2016**, **14**, 851–858

Special Issue in honor of Dr. Serge Kaliaguine

Résumé

La production d'hydrogène à partir de la décomposition de l'eau par des réactions photocatalytiques peut être une énergie propre, alternative aux combustibles fossiles dans le futur. Le nitrure graphitique de carbone (g-C_3N_4) est l'un des photocatalyseurs actifs dans la région visible du spectre lumineux qui peut être combiné avec d'autres semi-conducteurs afin d'augmenter son efficacité photocatalytique. Le TiO_2 est l'un des choix les plus appropriés à combiner avec g-C_3N_4 en raison de l'intervalle entre ses bandes de valence et de conduction et de ses diverses formes de nanostructures existantes. Dans ce travail, des nano feuilles de g-C_3N_4 ont été mélangés avec des nanoparticules d'oxyde de titanate afin d'améliorer la séparation des charges et l'efficacité photocatalytique de la structure. En conséquence, le rendement de ce nouveau nanocomposite vis-à-vis de la production de dihydrogène est presque deux fois celui du g-C_3N_4 pure.

Abstract

Hydrogen production from water splitting via photocatalytic reactions can be an alternative clean energy of fossil fuels in the future. Graphitic carbon nitride (g-C_3N_4) is one of the photocatalysts active in the visible light region that can be combined with other semiconductors in order to increase its photocatalytic efficiency. TiO_2 is one of the most appropriate choices to combine with g-C_3N_4 because of its conduction band edge and variety forms of nanostructures. In this work, nanosheets of g-C_3N_4 were mixed with nanoparticles of titanate in order to enhance charge separation and photocatalytic efficiency. Consequently, the hydrogen evolution of this novel nanocomposite produced almost twice as much hydrogen in comparison with g-C_3N_4.

4.1 Introduction

Fossil fuels provide the cheapest source of energy for human beings, in spite of their environmental issues such as: air pollution and CO_2 emissions, which causes to global warming and climate change. As a matter of fact, energy demands are increasing annually and so fossil fuels are used more quickly than before. However, the resources of this kind of energy are limited and we may face an energy crisis in the near future.

Scientists believe that solar energy is one of the best alternatives to substitute for fossil fuels because it is abundant, renewable and environmentally friendly. It is estimated that the worldwide energy consumption of one year can be produced by only 0.01% of sunlight irradiation during one second.[17, 58, 77] However, the most important concern of this energy resources is how to utilize it into practical applications. It has been suggested that utilizing hydrogen as an energy carriers not only solves these problems, but can also reduce air pollution. [30, 311] Moreover, water is the only product from hydrogen combustion and so there are no CO_2 emissions during hydrogen consumption.

In 1972, Fujishima and Honda made the discovery that TiO_2 and Pt could split water into hydrogen and oxygen under UV light illumination.[6] Since then, researchers have tried to synthesize photocatalysts that can produce hydrogen from water under sunlight irradiation. However, the majority of sunlight illumination is in the visible light region and so efficient photocatalysts should be activated under visible light irradiation (400-700 nm).[27]

Graphitic carbon nitride (g-C_3N_4) is one of the best visible light active photocatalyst that has attracted much of interest, recently.[142, 312, 313] Wang et al. showed that g-C_3N_4 can be excited under visible light irradiation and produce hydrogen from a mixture of water and a sacrificial reagent.[151] They used triethanolamine as an electron scavenger and Pt as a cocatalyst. Later many researchers have tried to improve its efficiency by introducing various methods such as doping with other elements, applying different cocatalysts, making nanosheets of g-C_3N_4 and creating carbon nitride based nanocomposites.[314] In this work, a nanocomposite of g-C_3N_4 nanosheets and titanate nanodisks (TNDs) is proposed in order to increase charge separation and so enhance hydrogen production under visible light illumination. Titanate nanodisks were synthesized according to previous reports. [89, 308] These nanoparticles of TiO_2 have lower conduction band in comparison with g-C_3N_4 and so excited electron can transfer from g-C_3N_4 to

TiO_2.[315] Meanwhile, excited holes remain in g-C_3N_4 valence band and as a result charge recombination phenomenon is partially prohibited and the photocatalyst efficiency for hydrogen production increases.

4.2 Experimental

4.2.1 Carbon nitride bulk material

Graphitic carbon nitride was produced from melamine as reported previously. [309, 310] Briefly, 10 g melamine was heated in a crucible to 550 °C and kept at this temperature for 3 h. Then, the obtained yellow powder was ground and washed with water and ethanol several times. It was, then, dried thoroughly in an oven at 70 °C.

4.2.2 Carbon nitride nanosheet by liquid exfoliation

After synthesizing bulk g-C_3N_4, nanosheets of carbon nitride were made by liquid exfoliation (denoted as g-C_3N_4-LE).[154, 169] Typically, 1 g of bulk material was added to a mixture of 100 ml isopropanol and 100 ml water. Then, the mixture was sonicated for 12 h. Nanosheets were, then, separated from residual bulk material (aggregates) by centrifugation at 3000 rpm for 10 min. Then, the obtained nanosheets were centrifuged at 10000 rpm for 15 min and dried at 70 °C.

4.2.3 Carbon nitride nanosheets by gas template

Nanosheets of g-C_3N_4 were synthesized by one step method called gas template (denoted as g-C_3N_4-GT) according to the method reported in ref. [167]. First, 15 g of ammonium chloride was dissolve in 200 ml of water and then 3 g melamine was added to the mixture. Later, it was heated to 60 °C in order to remove water and then, it was dried in an oven at 70 °C. Once this step is completed, the white powder was heated at 550 °C for 4 h in a semi-closed system. During the calcination process, ammonium chloride acts as a dynamic gas template, helping to synthesize ultrathin g-C_3N_4.[167] After this stage, the resultant nanosheets were washed several times with ethanol and water and dried in an over.

4.2.4 Titanate nanodisks

TNDs were prepared by a solvothermal method described in our previous work.[308] Briefly, 3.4g of titanium butoxide was added to a mixture of 20g oleylamine and 20g benzyl alcohol. Then, 90g benzyl ether was added to the mixture and all of them were transfer to a round-bottom flask. The flask was kept in an oven at 180 °C for 24 h. After cooling down, the obtained TNDs were washed completely with toluene and ethanol and were treated with tetraethylammonium hydroxide in order to obtain water-soluble TEA-TNDs. As a result, TNDs with ability to disperse in water were obtained (Figure 4.1). These highly uniform nanoparticles with an average diameter of 35 nm can be utilized on the surface of g-C_3N_4 nanosheets. Therefore, charge separation between TND and nanosheets of g-C_3N_4 become more effective because of their very small size and high g-C_3N_4/TNDs interface.

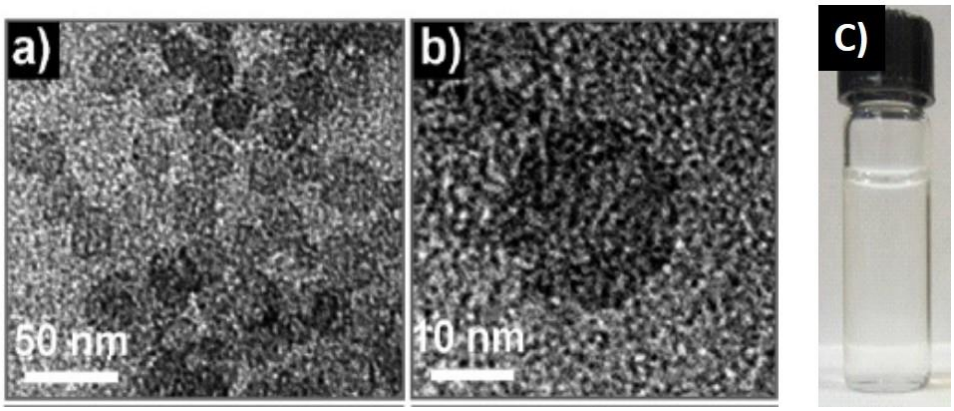

Figure 4.1. TEM pictures of TNDs (a), (b) and photograph of highly dispersed TNDs in water (c)

4.2.5 Nanocomposite of g-C_3N_4 nanosheets and TNDs

After synthesizing TNDs and g-C_3N_4 nanosheets, both nanomaterials were mixed together with the ratio of 30 wt% TNDs as follows. The pH of nanosheets was decreased in order to make the surface positive charges.[310] Due to the negative charge surface of TNDs, both nanoparticles can make better contact at lower pH. The mixture was heated under agitation until it dried. After that, the obtained powder was calcined at 400 °C for 3 h to obtain a g-C_3N_4/TiO_2 nanocomposite. Owing to the particle size of TNDs (20 nm), they deposited on the surface of g-C_3N_4 nanosheets.[316] Then, Pt metal nanoparticles were deposited on the surface of the nanocomposite

via photodeposition technique under visible light irradiation.[317] Although Pt nanoparticles are partially deposited on both surfaces of semiconductors, those that deposited on the TiO_2 nanoparticles have more ability to enhance charge separation and so hydrogen generation would be increased.

4.2.6 Characterization

Transmission electron microscopy (TEM) images of the samples were obtained on a JOEL JEM 1230 operated at 120kV. Powder X-ray diffraction (XRD) patterns of the samples were obtained on a Bruker SMART APEXII X-ray diffractometer equipped with a Cu Kα radiation source (λ=1.5418 Å). The UV-vis spectra were recorded on a Cary 300 Bio UV-visible spectrophotometer. Fourier transform infrared (FTIR) absorption spectra were measured with a FTS 45 infrared spectrophotometer with the KBr pellet technique.

4.2.7 Photocatalytic test

The photocatalytic reactions were performed in a gas-tight 10 ml Pyrex reaction cell as follows: 5 mg of the typical synthesized nanocomposite photocatalysts were dispersed in 5 ml aqueous solution of 10 wt% of triethanolamine. An adequate amount of chloroplatinic acid (H_2PtCl_6) was, then, dissolved directly in the above mixture in order to get 2 wt% of Pt, which acts as a cocatalyst and deposited by an in-situ photodeposition technique. After this stage is completed, the cell was evacuated and then purged with nitrogen for 10 min in order to eliminate dissolved oxygen. Then, the mixture was illuminated with a 300W Xe arc lamp equipped under stirring condition to prevent particles from settling at the bottom of the cell. A 0.5 mL of gas was sampled intermittently through septum, and hydrogen was analyzed by gas chromatography equipped with TCD detector and carboxen-1010 capillary column.

4.3 Results and discussions

4.3.1 Sample characterizations

The crystal structure of bulk carbon nitride and the obtained nanosheets from liquid exfoliation and gas template were characterized by XRD (Figure 4.2). According to the XRD results, the peaks in our samples can be indexed to g-C_3N_4. The strongest peak around 27.5° is characterized as (002) peak and related to the interlayer stacking peak of aromatic system.[151] It should be noted that this peak noticeably decrease, showing that g-C_3N_4 nanosheets were obtained. [154, 318] The other peak around 13° is indexed as (100) plane and is attributed to inter-planar structure of tri-s-triazine with a distance of about 0.675 nm. It is not surprising that after calcination a nanocomposite of g-C_3N_4 nanosheets and TNDs, the TNDs being converted to TiO_2 nanoparticles that cannot be detected by XRD, due to their small particle sizes, good dispersion and weak crystallinity.[319] The optical absorption spectra for graphitic carbon nitride and nanosheets are shown in Figure 4.3. The results showed that all the samples are semiconductors with the strong visible light absorption ability in the range of 400 to 550 nm. As can be seen in Figure 4.3, nanosheets of g-C_3N, due to the quantum confinement effect, their band gaps increased and the UV-visible curve shifted to shorter wavelengths and so they could absorb less visible light. The differences between UV-visible spectra of nanosheets from liquid exfoliation (LE) and gas template (GT) methods, indicated that the nanosheets of g-C_3N_4-GT were thinner than g-C_3N_4-LE. Furthermore, the band gap energies of all samples, which were estimated from the intercept of the tangents to the plot of $(Ah\nu)^{1/2}$ vs. photon energy, proved the same results.[320, 321] As it is calculated the band gap of bulk graphitic carbon nitride is 2.70 eV, which is in good agreement with the literature (Figure 4.4-a).[151] As it is demonstrated in Figure 4.4-b,c, the band gap energies of nanosheets synthesized from liquid exfoliation technique and gas template approach, are 2.74 and 2.76 eV, respectively. In other words, by obtaining nanosheet structure of g-C_3N_4 due to the quantum confinement effect, the band gap increased and it could absorb less visible light.

The molecular structure of the synthesized sample is investigated by FT-IR spectra, as shown in Figure 4.5. The broad band between 3000 and 3500 cm^{-1} can be related to N-H stretching and

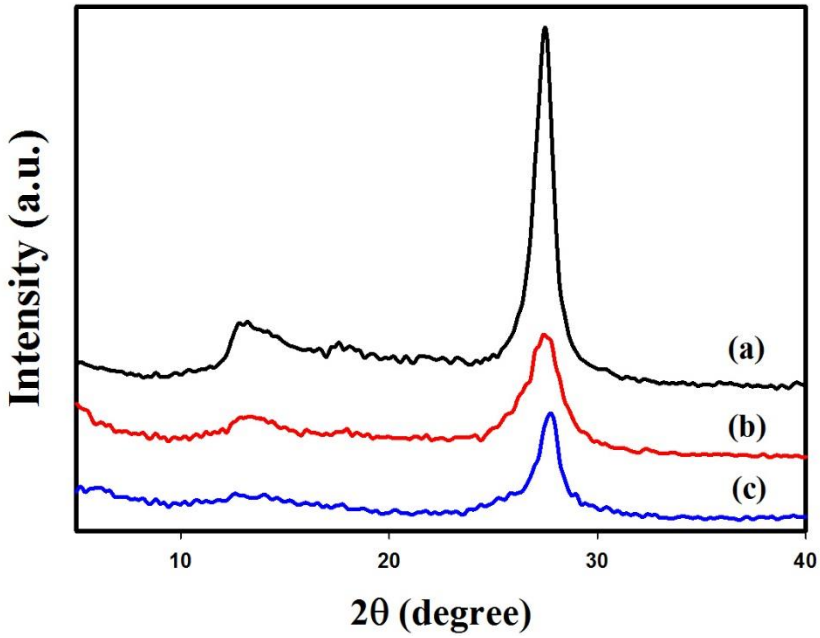

Figure 4.2. XRD pattern of (a) g-C_3N_4 in bulk; (b) and (c) g-C_3N_4 nanosheets prepared by gas template and liquid exfoliation, respectively.

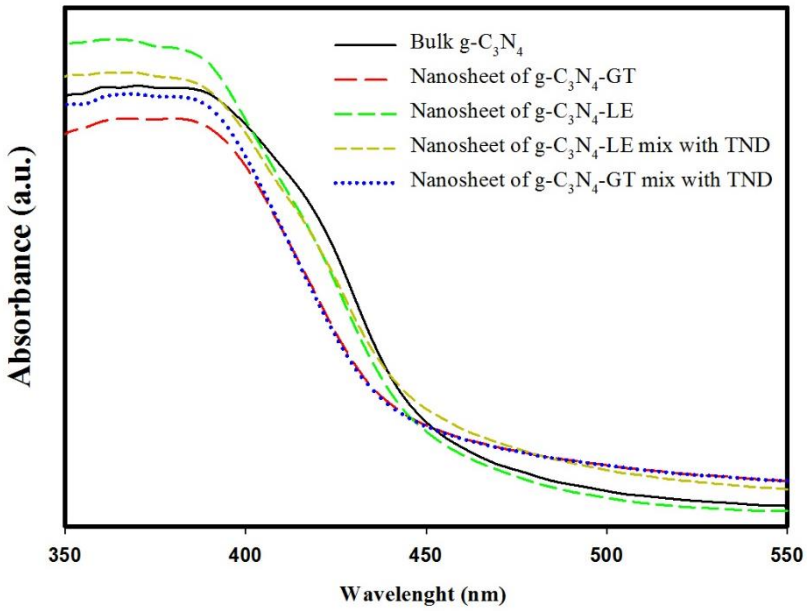

Figure 4.3. UV-visible absorption spectra of g-C_3N_4 bulk, g-C_3N_4 nanosheets prepared by gas template and liquid exfoliation, and nanosheets with TND before calcination

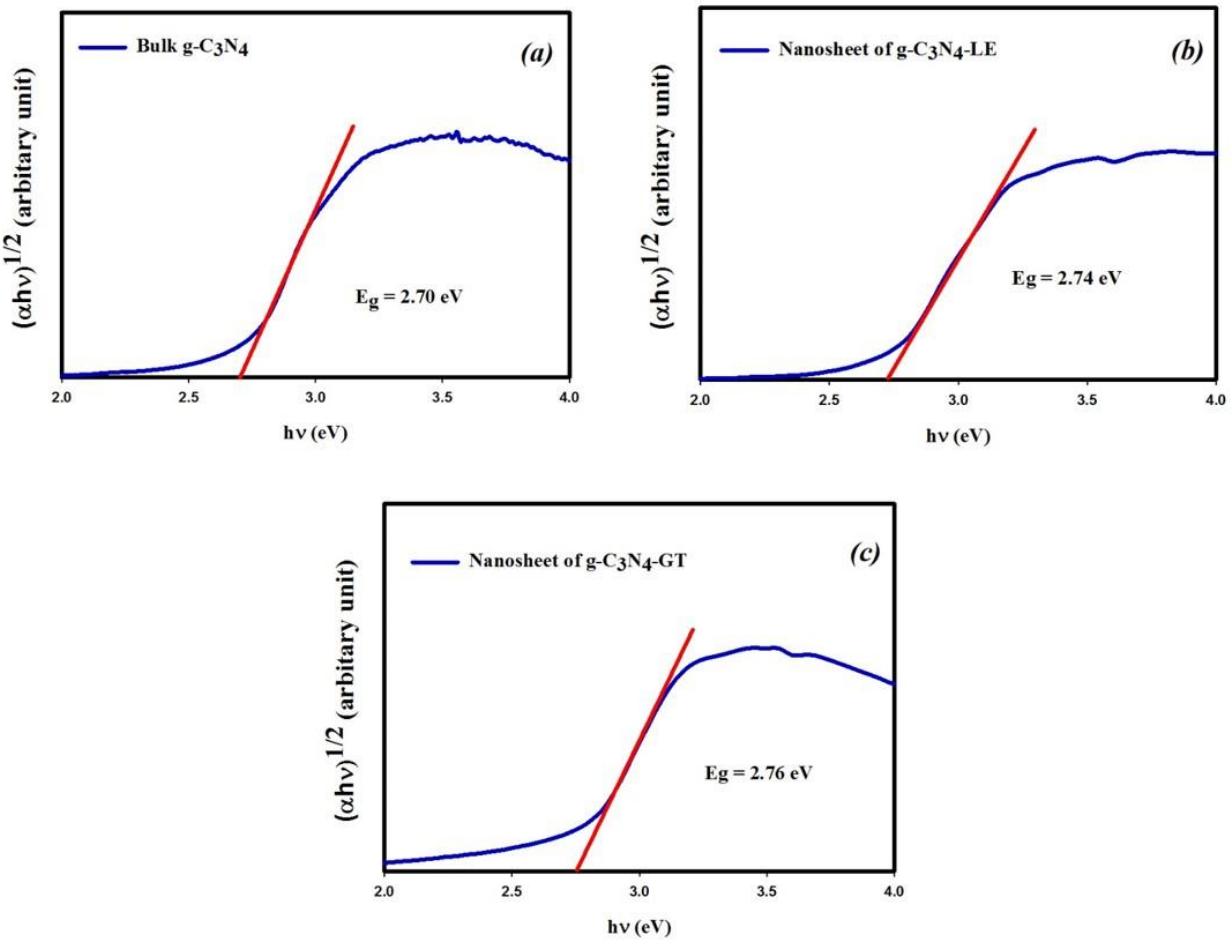

Figure 4.4. The estimated band gap energy of (a) bulk g-C_3N_4 (b) g-C_3N_4 nanosheet via liquid exfoliation method (c) g-C_3N_4 nanosheet via gas template method

and some absorbed water molecules. [229, 322] Some strong bands were observed at 1570-1634 cm^{-1} is owing to the presence of C=N and the peaks showed in the range of 1258-1480 cm^{-1} can be attributed to stretching modes of C-N heterocycles.[322] Some strong bands were observed at 1570-1634 cm^{-1} is owing to the presence of C=N and the peaks showed in the range of 1258-1480 cm^{-1} can be attributed to stretching modes of C-N heterocycles.[322] Moreover, the vibration in the region of 810-880 cm^{-1} corresponds to triazine unit characteristic of the chemical g-C_3N_4 structure [145, 323]

The nitrogen adsorption-desorption isotherms of the different samples are presented in Figure 4.6. As can be seen, they all are type IV, according to IUPAC classification, showing mesopores materials. [310, 316] The hysteresis loop of nanocomposite of g-C_3N_4 and TiO_2 becomes larger

and shifts to the lower pressure region in comparison to g-C_3N_4 nanosheets. This reveals that relatively larger mesopores are created during synthesis of the nanocomposite. Based on BET analysis the specific surface area of the nanocomposite is 75 m^2/g, which is higher than that of bulk g-C_3N_4 material (21 m^2/g) and g-C_3N_4 nanosheets (63 m^2/g).

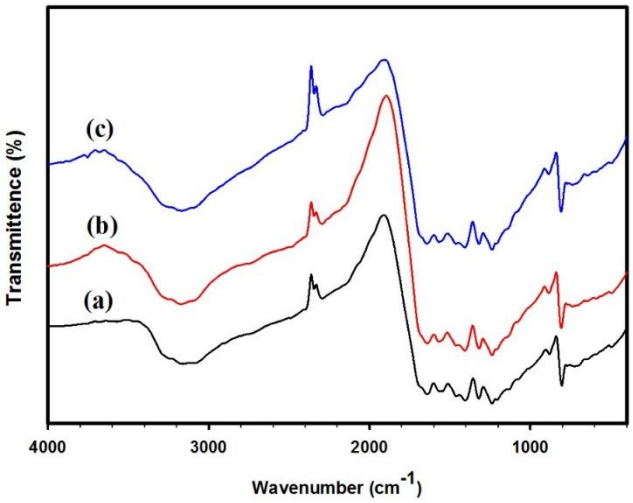

Figure 4.5. FTIR spectra of (a) bulk g-C_3N_4 and (b) and (c) g-C_3N_4 nanosheets obtained by liquid exfoliation and gas template, respectively.

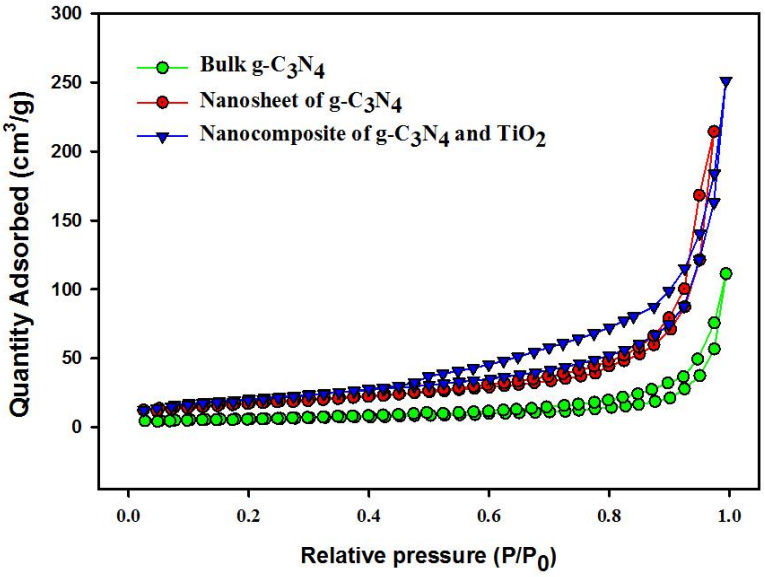

Figure 4.6. Nitrogen adsorption-desorption isotherms for the g-C_3N_4 bulk, g-C_3N_4 nanosheets, and g-C_3N_4/TiO_2 nanocomposite.

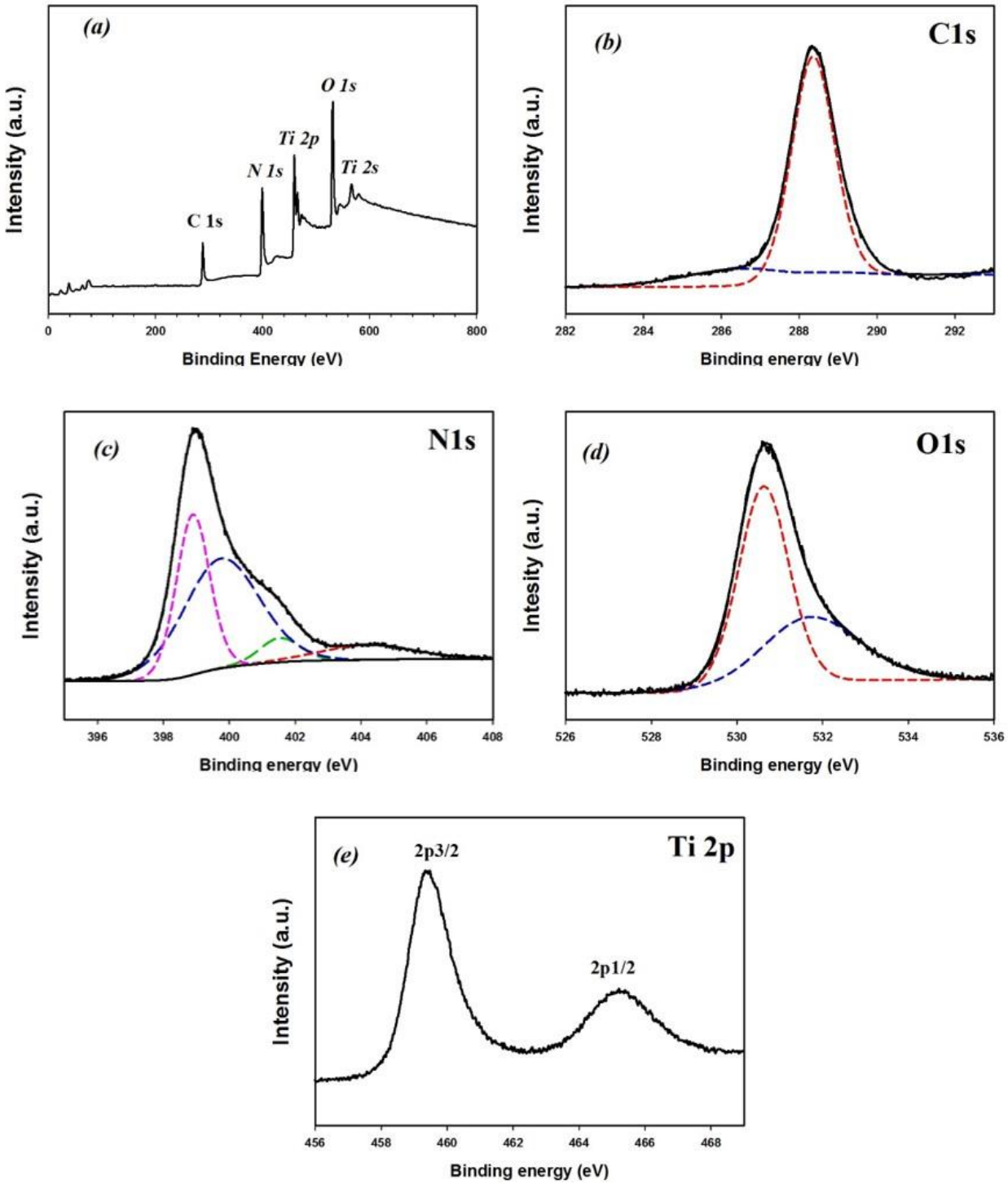

Figure 4.7. XPS survey spectrum of (a) the g-C_3N_4-TiO_2 nanocomposite. High resolution XPS spectra of (b) C 1s, (c) N 1s, (d) O 1s and (e) Ti 2p of the g-C_3N_4-TiO_2 nanocomposite.

Figure 4.7 displays XPS analysis of the g-C_3N_4/TiO_2 nanocomposites. As shown in Figure 4.7-a, the obtained nanocomposite consists of C, N, O and Ti which are located at binding energies of 288, 399, 530 and 459 eV, respectively. The high-resolution XPS spectrum of C 1s shown in Figure 4.7-b, can be fitted into two peaks at 286.1 and 288.4 eV, that are related to the C–N–C and the C–$(N)_3$ group of graphitic carbon nitride.[143, 324] The XPS spectrum of N 1s (Figure 4.7-c) can be ascribed to four different kinds of bonds as follows: C=N–C at 398.8 eV, tertiary nitrogen $(C)_3$–N at 399.7, N–H at 401.4 and π–excitation at 404.4.[310, 324] As illustrated in Figure 4.7-d, the O1s XPS spectrum can be deconvoluted into two main energy values of 530.6 and 531.8.[143] The first peak is associated with the O^{2-} in the TiO_2 and the other one is attributed of –OH bands on the nanocomposite surface. [315, 319, 325] The XPS Ti 2p high-resolution analysis (Figure 4.7-e) displays two main peaks at 459.4 and 465.1 related to binding energy of Ti $2p_{3/2}$ and $2p_{1/2}$, respectively, and are characteristic of Ti^{4+}.[316, 325]

4.3.2 Photocatalytic activity of nanocomposite for hydrogen production

Figure 4.8 displays hydrogen production under visible light illumination after 3 h. As it can be seen, the nanocomposites showed higher hydrogen evolution in comparison with pristine nanosheets of g-C_3N_4 prepared by two different methods (all samples containing 2 wt% Pt as a cocatalyst). Although both nanosheets of g-C_3N_4-LE and g-C_3N_4-GT produced about the same amount of hydrogen (734 and 726 μmol h^{-1} g^{-1}cat, respectively) after 3 h under visible light irradiation, their nanocomposites showed slightly different behaviours. As it is shown, the nanocomposite of g-C_3N_4-LE/TiO_2(70:30 wt%) could generate 1633 μmol h^{-1} g^{-1}cat of hydrogen, while the nanocomposite of g-C_3N_4-GT/TiO_2(70:30 wt%)produced 1886 μmol h^{-1} g^{-1}cat. This can be attributed to the higher surface area of g-C_3N_4-GT nanosheets and closer contact with TiO_2 nanoparticles. [167] According to the results of photocatalytic tests (Figure 4.8), the optimum amount of TiO_2 should be 30 wt%. Although 10 wt% loading of TiO_2 in the nanocomposite can improve charge separation as described in the next section, this amount is not sufficient to acquire the maximum hydrogen generation. Furthermore, by depositing 50 wt% of TiO_2 on the surface of g-C_3N_4 nanosheets, more surface of g-C_3N_4 is covered by TiO2 nanoparticle and so the visible light absorption of g-C_3N_4 is declined and as a result the hydrogen production is reduced significantly.[143]

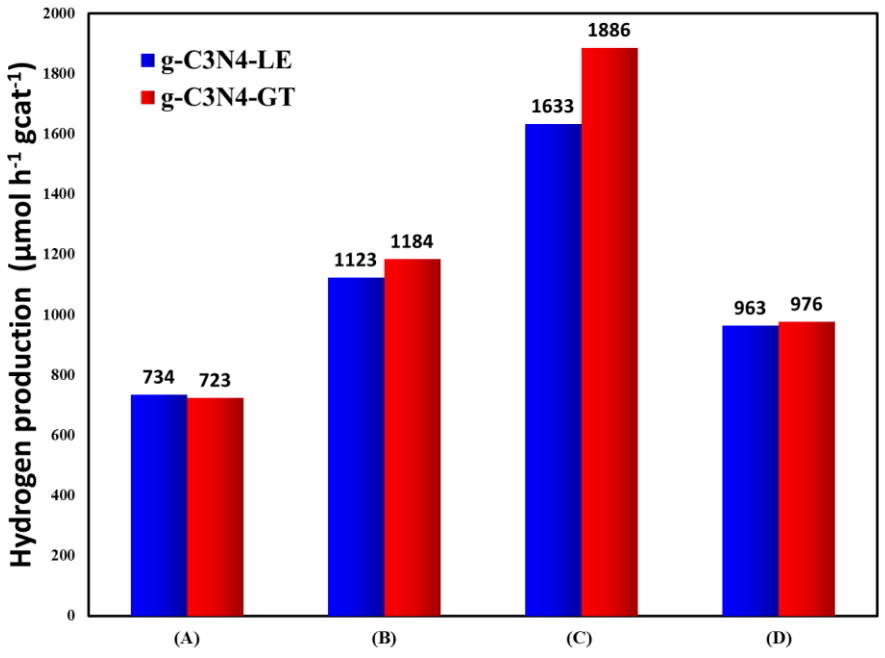

Figure 4.8. Hydrogen production of different nanocomposite under visible light irradiation after 3 h: (A) g-C_3N_4 nanosheets without TiO_2, (B) g-C_3N_4 nanosheets with 10wt% TiO_2, (C) g-C_3N_4 nanosheets with 30wt% TiO_2 and (D) g-C_3N_4 nanosheets with 50wt% TiO_2.

The mechanism of hydrogen production improvement of this nanocomposite is demonstrated in Figure 4.9.First, g-C_3N_4 nanosheet absorbs the photon energy of visible light and produces excited electrons and holes, which are generated in the conduction and valence bands, respectively. Because of ultrathin g-C_3N_4 nanosheets (thickness ~ 1-3 nm), photoexcited charge carriers can easily transfer to the surface of g-C_3N_4. Although excited holes remain on the g-C_3N_4 nanosheet valence band, photogenerated electrons can transfer from conduction band of g-C_3N_4 to TiO_2 nanoparticles because of lower conduction band edge of TiO_2 (as displayed in Figure 4.9). These electrons can move to Pt nanoparticles and reduce protons to hydrogen. As a result, photogenerated electrons and holes separate from each other and the probability of charge recombination declines significantly. Therefore, charge carriers in the proposed nanocomposite have longer lifetime than pristine g-C_3N_4 and so this nanocomposite could produce more hydrogen compared to g-C_3N_4 nanosheets.

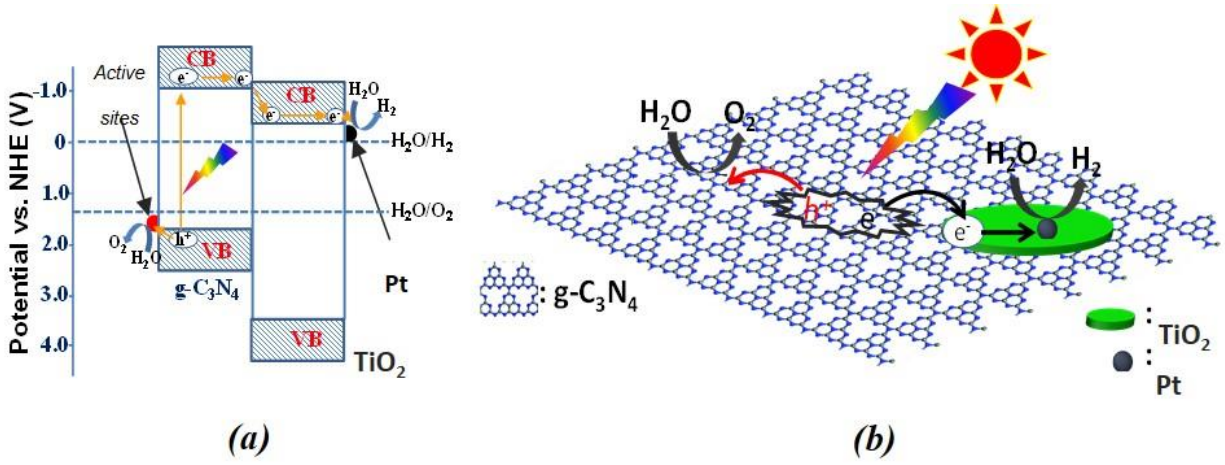

Figure 4.9. Schematic illustration of (a) potential energy diagram, (b) charge transfer in the nanocomposite of Pt-g-C_3N_4-TiO_2

4.4 Conclusion

Graphitic carbon nitride is a semiconductor that is activated under visible light illumination for hydrogen evolution from water. Many scientists have tried to improve its performance in order to obtain more hydrogen in the same conditions. One of the ways to gain more hydrogen is creation of novel nanocomposites of g-C_3N_4 with other semiconductors such as TiO_2. In this research, a nanocomposite of g-C_3N_4 nanosheets and titanate nanodisks (TNDs) has been proposed with the aim of raising hydrogen evolution efficiency. After synthesizing various nanosheets of g-C_3N_4 from different methods, TNDs were introduced by the impregnation technique. After drying and calcination, this nanocomposite showed almost doubled hydrogen production under visible light illumination which resulted from a better charge separation between g-C_3N_4 and TNDs. Therefore, charge recombination is partially prevented and so more excited electrons can react with protons and generate hydrogen molecules.